

Fano feature induced by a bound state in the continuum via resonant state expansion

Pavel S. Pankin^{1,2,+,*}, Dmitrii N. Maksimov^{1,2,+}, Kuo-Ping Chen³, and Ivan V. Timofeev^{1,2}

¹Kirensky Institute of Physics, Federal Research Center KSC SB RAS, 660036, Krasnoyarsk, Russia

²Siberian Federal University, 660041, Krasnoyarsk, Russia

³Institute of Imaging and Biomedical Photonics, National Chiao Tung University, 71150, Tainan, Taiwan, ROC

*pavel-s-pankin@iph.krasn.ru

+these authors contributed equally to this work

ABSTRACT

We consider light scattering by an anisotropic defect layer embedded into anisotropic photonic crystal in the spectral vicinity of an optical bound state in the continuum (BIC). Using a resonant state expansion method we derive an analytic solution for reflection and transmission amplitudes. The analytic solution is constructed via a perturbative approach with the BIC as the zeroth order approximation. The solution is found to describe the collapsing Fano feature in the spectral vicinity of the BIC. The findings are confirmed via comparison against direct numerical simulations with the Berreman transfer matrix method.

1 Introduction

Theoretical insight into resonant response from optical systems, including photonic-crystalline resonators¹ and resonant metasurfaces², is of big importance in photonics^{3,4}. Very unfortunately only a few systems generally allow for a tractable analytic solution providing intuitively clear and mathematically exact picture, such as, e.g., the celebrated Mie-Lorenz theory⁵. Thus, in the field of optics the resonant scattering quite often can only be understood in terms of the temporal coupled mode theory (TCMT)⁶⁻⁸. The TCMT is a phenomenological approach that maps the scattering problem onto a system of field driven lossy oscillators. Mathematically, the problem is cast in the form of a system of linear differential equations. The coefficients of the system account for both "internal" modes of the resonant structure as well as for the coupling of the "internal" modes to incoming and outgoing waves. The interaction with the impinging light is understood in terms of "coupled modes" which are populated when the system is illuminated from the far-zone. The elegance of the TCMT is in its simplicity and the relative ease in establishing important relationships between the phenomenological coefficients solely from the system's symmetries and conservation laws⁷⁻¹⁰. However, despite its numerous and successful applications, the TCMT generally relies on a set of fitting parameters. Moreover, the mathematical foundations of the TCMT remain vague since the theory neither gives an exact definition of the "coupled mode", nor a clear recipe for such a "coupled mode" to be computed numerically.

Historically, the problem of coupling between the system's eigenmodes to the scattering channels with the continuous spectrum has attracted a big deal of attention in the field of quantum mechanics¹¹⁻¹³. One of the central ideas was the use of the Feshbach projection method^{12,14} for mapping the problem onto the Hilbert space spanned by the eigenstates of the scattering domain isolated from the environment. Such approaches have met with a limited success in application to various wave related set-ups, including quantum billiards¹⁵⁻¹⁷, tight-binding models¹⁸, potential scattering¹⁹, acoustic resonators²⁰, nanowire hetrostructures²¹ and, quite recently, dielectric resonators²². Besides its mathematical complexity there are two major problems with the Feshbach projection method: First, the eigenmodes of the isolated systems are in general not known analytically; therefore, some numerical solver has most often to be applied. Furthermore, the computations of such eigenmodes requires some sort of artificial boundary condition on the interface between the scattering domain and the outer space. Quite remarkably the convergence of the method is shown to be strongly affected by the choice of the boundary condition on the interface^{16,23,24}.

In the recent decades we have witnessed the rise of efficient numerical solvers utilizing perfectly matched layer (PML) absorbing boundary conditions^{25,26}. The application of perfectly matched layer has rendered numerical modelling of wave propagation in open optical, quantum, and acoustic systems noticeably less difficult allowing for direct full-wave simulations even in three spatial dimensions. On the other hand, the application of PML also made it possible to compute the eigenmodes and eigenfrequencies of wave equations with reflectionless boundary conditions. Such eigenmodes come under many names including quasinormal modes⁴, Gamow states²⁷, decaying states²⁸, leaky modes²⁹, and resonant states³⁰. The availability of the resonant states has naturally invited applications to solving Maxwell's equations via series expansions giving rise to a

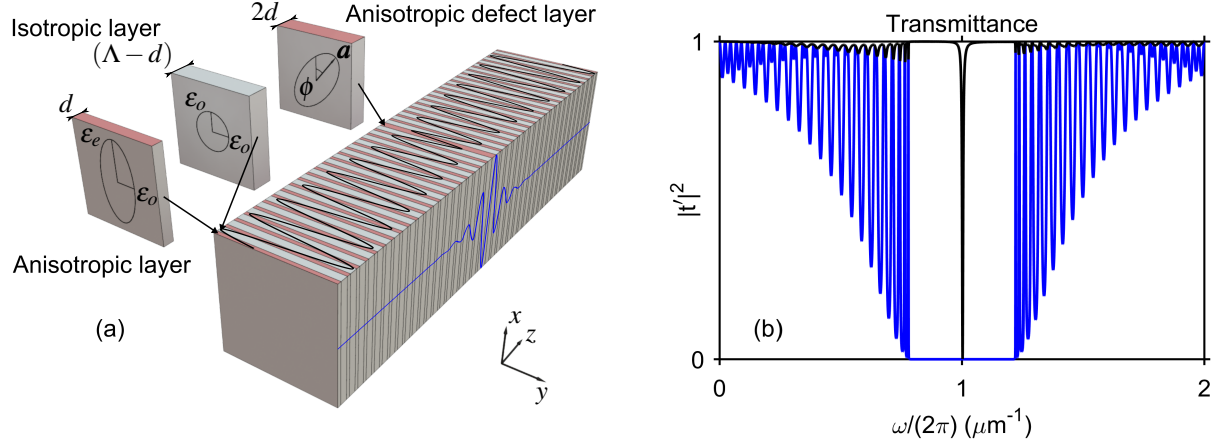


Figure 1. (a) One-dimensional PhC structure stacked of alternating layers of an isotropic dielectric material with permittivity ϵ_o (gray) and an anisotropic material with the permittivity components ϵ_o and ϵ_e (pink). An anisotropic defect layer with a tuneable permittivity tensor is inserted in the center of the structure. The analytic solution for the quasi-BIC mode profile is plotted on top and right sides of the stack: the x -wave component $\text{Re}(E_x)$ – blue, the y -wave component $\text{Re}(E_y)$ – black. (b) The transmittance spectra $|t'|^2$ of x - (blue) and y -waves (black) for PhC structure from Fig. 1(a) calculated with Berreman’s method. The parameters are $\epsilon_e = 4$, $\epsilon_o = 1$, $d = 0.125 \mu\text{m}$, $(\Lambda - d) = 0.250 \mu\text{m}$, tilt angle $\phi = \pi/9$ (a), $\phi = \pi/18$ (b).

variety of resonant state expansion (RSE) methods⁴. One problem with the resonant states is that they are not orthogonal in the usual sense of convolution between two mode shapes with integration over the whole space^{13,31}. This can be seen as a consequence of exponential divergence with the distance from the scattering center⁴. Fortunately, both of the normalization and orthogonality issues have recently been by large resolved with different approaches, most notably through the PML³², and the flux-volume (FV)^{28,30} normalization conditions.

In this paper we propose a RSE approach to the problem of light scattering by an anisotropic defect layer (ADL) embedded into anisotropic photonic crystal (PhC) in the spectral vicinity of an optical BIC. Although BICs are ubiquitous in various optical systems^{33,34}, the system under scrutiny is the only one allowing for an exact full-wave analytic solution for an optical BIC³⁵. By matching the general solution of Maxwell’s equation within the ADL to both evanescent and propagating solutions in the PhC^{50–53} we find the eigenfield and eigenfrequency of the resonant mode family limiting to the BIC under variation of a control parameter. Next, for finding the scattering spectra we apply the spectral representation of Green’s function in terms the FV-normalized resonant states³⁰. This is a well developed approach which has already been applied to both two³⁶- and three³⁷-dimensional optical systems. The approach has also been recently extended to magnetic, chiral, and bi-anisotropic optical materials³⁸ as well as potential scattering in quantum mechanics³⁹. Remarkably, so far RSE methods have been mostly seen as a numerical tool. Here we show how a perturbative analytic solution can be constructed in a closed form within the RSE framework. Such a perturbative solution uses the BIC as the zeroth order approximation and, very importantly, is capable of describing the collapsing Fano resonance^{40–45} in the spectral vicinity of the BIC. We mention in passing that due to the fine control of Fano line-shapes optical BICs has been recently viewed as an efficient instrument in design of narrowband optical filters^{46–49}. We shall see that the analytic solution matches the exact numerical result to a good accuracy.

2 The System

The system under scrutiny is composed of an ADL with two anisotropic PhC arms attached to its sides as shown in Fig. 1 (a). Each PhC arm is a one-dimensional PhC with alternating layers of isotropic and anisotropic dielectric materials. The layers are stacked along the z -axis with period Λ . The isotropic layers are made of a dielectric material with permittivity ϵ_o and thickness $\Lambda - d$. The thickness of each anisotropic layer is d . The anisotropic layers have their principal dielectric axes aligned with the x , y -axes with the corresponding permittivity component principal dielectric constants ϵ_e , ϵ_o , but the principal axes of the ADL are tilted with respect of the principal axes of the PhC arms as shown in Fig. 1(a). Propagation of the monochromatic electromagnetic waves is controlled by Maxwell’s equations of the following form³⁵

$$\begin{Bmatrix} 0 & \nabla \times \\ -\nabla \times & 0 \end{Bmatrix} \begin{Bmatrix} \mathbf{E} \\ \mathbf{H} \end{Bmatrix} = -ik_0 \begin{Bmatrix} \hat{\epsilon} \mathbf{E} \\ \mathbf{H} \end{Bmatrix}, \quad (1)$$

where \mathbf{E} is the electric vector, \mathbf{H} is the magnetic vector, $k_0 = \omega/c$ is the wave number in vacuum with c as the speed of light, and, finally, $\hat{\epsilon}$ is the dielectric tensor. The orientation of the ADL optical axis is determined by the unit vector

$$\mathbf{a} = \{\cos(\phi), \sin(\phi), 0\}^\dagger, \quad (2)$$

as shown in Fig. 1(a). Since the reference frame is aligned with the optical axes in the PhC, the dielectric tensor is diagonal everywhere out of the ADL. Given that \mathbf{a} is specified by the tilt angle ϕ , in the ADL it takes the following form

$$\hat{\epsilon} = \begin{Bmatrix} \epsilon_e \cos^2(\phi) + \epsilon_o \sin^2(\phi) & \sin(2\phi) (\epsilon_e - \epsilon_o)/2 \\ \sin(2\phi) (\epsilon_e - \epsilon_o)/2 & \epsilon_e \sin^2(\phi) + \epsilon_o \cos^2(\phi) \end{Bmatrix}. \quad (3)$$

In this paper we restrict ourselves with the normal incidence, i.e. the Bloch wave vector is aligned with the z -axis in Fig. 1(a). The dispersion of waves in the PhC arms depends on polarization. For the x -polarized waves (x -waves) the dispersion relationship is that of a one-dimensional PhC⁵⁰⁻⁵³

$$\cos(K\Lambda) = \cos(k_e d) \cos[k_o(\Lambda - d)] - \frac{1 + r_{oe}^2}{1 - r_{oe}^2} \sin(k_e d) \sin[k_o(\Lambda - d)], \quad (4)$$

where K is the Bloch wave number,

$$k_e = k_0 \sqrt{\epsilon_e} = k_0 n_e, \quad k_o = k_0 \sqrt{\epsilon_o} = k_0 n_o, \quad (5)$$

and the Fresnel coefficient r_{oe} is given by

$$r_{oe} = \frac{k_o - k_e}{k_o + k_e}. \quad (6)$$

Equation (4) defines the band structure for the x -waves with the condition $|\cos(K\Lambda)| = 1$ corresponding to the edges of the photonic band gap in which the wave propagation is forbidden. In Fig. 1 (a) we demonstrate the transmittance spectrum of the system with 20 bi-layers in each PhC arms; the overall system being submersed in air. One can see that for the x -waves the transmittance is zero within the band gap. On the other hand the PhC arms are always transparent to the y -polarized waves (y -waves) with dispersion $k_o = \epsilon_o k_0$. Notice, though, that the y -waves transmittance exhibits a sharp dip at the center of the band gap. This dip is due to a high quality resonant mode predicted in³⁵. Although the line shape is symmetric, the dip, nonetheless, can be attributed to a Fano resonance as the transmittance reaches zero at the center of the band gap indicating a full destructive interference between two transmission paths. In this paper we set a goal of finding the analytic solution describing the Fano anomaly in the band gap.

3 Resonant eigenmode and bound state in the continuum

The resonant states are the eigenmodes of Maxwell's equations (1) with reflectionless boundary conditions in the PhC arms. The equation for resonant eigenfrequencies can be obtained by matching the general solution in the ADL to the outgoing, both propagating and evanescent, waves in the PhC arms. Let us start from the general solution in the ADL.

3.1 General solution in the ADL

First, the unit vector along the propagation direction is defined as

$$\boldsymbol{\kappa}^{(\pm)} = [0, 0, \pm 1], \quad (7)$$

where the symbol \pm is used to discriminate between forward and backward propagating waves with respect to the orientation of the z -axis. The ADL supports two types of electromagnetic waves of different polarization. The e -waves with wavenumber $k_e = \epsilon_e k_0$ are polarized along the director \mathbf{a} , equation (2), while the o -waves with wavenumber $k_o = \epsilon_o k_0$ have their electric vector perpendicular to both \mathbf{a} and $\boldsymbol{\kappa}$, as seen from Fig. 1. The electric and magnetic vectors of the e -wave can be written as

$$\mathbf{E}_e^{(\pm)} = E_e^{(\pm)} \mathbf{a}, \quad \mathbf{H}_e^{(\pm)} = \frac{k_e}{k_0} [\boldsymbol{\kappa}^{(\pm)} \times \mathbf{E}_e^{(\pm)}], \quad (8)$$

where $E_e^{(\pm)}$ are unknown amplitudes. At the same time for o -waves we have

$$\mathbf{E}_o^{(\pm)} = E_o^{(\pm)} [\mathbf{a} \times \boldsymbol{\kappa}^{(\pm)}], \quad \mathbf{H}_o^{(\pm)} = \frac{k_o}{k_0} [\boldsymbol{\kappa}^{(\pm)} \times \mathbf{E}_o^{(\pm)}], \quad (9)$$

where $E_o^{(\pm)}$ are again unknown amplitudes. The general solution of equations (1) in the ADL, $z \in [-d, d]$, is written as a sum of the forward and backward propagating waves

$$\mathbf{E} = \sum_{j=o,e} \left(\mathbf{E}_j^{(+)} e^{ik_j z} + \mathbf{E}_j^{(-)} e^{-ik_j z} \right), \quad \mathbf{H} = \sum_{j=o,e} \left(\mathbf{H}_j^{(+)} e^{ik_j z} + \mathbf{H}_j^{(-)} e^{-ik_j z} \right). \quad (10)$$

3.2 General solution in the PhC arms

The general solution of Maxwell's equations (1) in the PhC arms is also written as a sum of forward and backward propagating waves. For the x -waves the field components E_x and H_y in the isotropic layer with the cell number m , $z \in [d + m\Lambda, (m + 1)\Lambda]$, are written as

$$\begin{aligned} E_x^{(m)} &= e^{iK\Lambda m} \left[A_x^{(+)} e^{ik_o(z-d-m\Lambda)} + A_x^{(-)} e^{-ik_o(z-d-m\Lambda)} \right], \\ H_y^{(m)} &= \frac{k_o}{k_0} e^{iK\Lambda m} \left[A_x^{(+)} e^{ik_o(z-d-m\Lambda)} - A_x^{(-)} e^{-ik_o(z-d-m\Lambda)} \right]. \end{aligned} \quad (11)$$

In the anisotropic layer with the cell number m , $z \in [(m + 1)\Lambda, d + (m + 1)\Lambda]$, we have

$$\begin{aligned} E_x^{(m)} &= e^{iK\Lambda m} \left[B_x^{(+)} e^{ik_e(z-m\Lambda-\Lambda)} + B_x^{(-)} e^{-ik_e(z-m\Lambda-\Lambda)} \right], \\ H_y^{(m)} &= \frac{k_e}{k_0} e^{iK\Lambda m} \left[B_x^{(+)} e^{ik_e(z-m\Lambda-\Lambda)} - B_x^{(-)} e^{-ik_e(z-m\Lambda-\Lambda)} \right]. \end{aligned} \quad (12)$$

By applying the continuity condition for the tangential field components the solutions (11) and (12) are matched on the boundary between the anisotropic layer in the $(m - 1)$ th cell and the isotropic layer in m th cell, $z = d + m\Lambda$, as well as on the boundary between the layers in the m th cell, $z = (m + 1)\Lambda$. This gives us a system of four equations for four unknowns, $A^{(+)}, A^{(-)}, B^{(+)}, B^{(-)}$. After solving for $B^{(+)}$ and $B^{(-)}$, this system can be reduced to the following two equations

$$\begin{cases} A^{(+)} \left[e^{ik_o(\Lambda-d)} - e^{iK\Lambda} e^{-ik_e d} \right] - A^{(-)} r_{oe} \left[e^{-ik_o(\Lambda-d)} - e^{iK\Lambda} e^{-ik_e d} \right] = 0, \\ -A^{(+)} r_{oe} \left[e^{ik_o(\Lambda-d)} - e^{iK\Lambda} e^{ik_e d} \right] + A^{(-)} \left[e^{-ik_o(\Lambda-d)} - e^{iK\Lambda} e^{ik_e d} \right] = 0, \end{cases} \quad (13)$$

where r_{oe} is given by equation (6). One can easily check that Eq. (13) is only solvable when K satisfies the dispersion relationship (4).

In contrast to the x -waves, for the outgoing y -waves in the right PhC arms the solution is simple

$$\begin{aligned} E_y &= -C^{(+)} e^{ik_o(z-d)}, \\ H_x &= \frac{k_o}{k_0} C^{(+)} e^{ik_o(z-d)}. \end{aligned} \quad (14)$$

Notice that so far we have not written down the solution in the left PhC arm. The direct application of that solution can be avoided by using the mirror symmetry of the system. Here, in accordance with ref³⁵ we restrict ourselves with the antisymmetric case

$$\mathbf{E}(z) = -\mathbf{E}(-z). \quad (15)$$

The generalization onto the symmetric case is straightforward.

3.3 Wave matching

Now we have all ingredients for finding the field profile of the antisymmetric resonant eigenmodes. By matching equation (10) to both equation (11) and equation (14) on the interface between the ADL and the right PhC arm and using equations (13, 15) one obtains eight equations for eight unknown variables $E_e^{(+)}, E_e^{(-)}, E_o^{(+)}, E_o^{(-)}, A^{(+)}, A^{(-)}, C^{(+)}, K$. After some lengthy and tedious calculations one finds that the system is solvable under the following condition

$$\frac{\xi e^{ik_o(\Lambda-d)} - r_{oe} e^{-ik_o(\Lambda-d)}}{\xi e^{-ik_e d} - r_{oe} e^{-ik_e d}} - \frac{e^{-ik_o(\Lambda-d)} - \xi r_{oe} e^{ik_o(\Lambda-d)}}{e^{ik_e d} - \xi r_{oe} e^{ik_e d}} = 0, \quad (16)$$

where

$$\xi = -e^{2ik_o d} \sin^2(\phi) + \frac{r_{oe} - e^{2ik_e d}}{1 - r_{oe} e^{2ik_e d}} \cos^2(\phi). \quad (17)$$

Taking into account equation (5) we see that the above formulae represent the transcendental equation for complex eigenvalues, k_0 of the Maxwell's equations (1). The analytic solution for the electromagnetic field within the ADL can be evaluated through

the following formulae

$$E_o^{(+)} = E_o^{(-)}, E_e^{(-)} = \zeta E_o^{(-)}, E_o^{(+)} = -\zeta E_o^{(-)}, E_o^{(-)} = \frac{iA}{2n_e \zeta},$$

$$\zeta = -\frac{e^{-ik_o d} t_{oe} \cos(\phi)}{(e^{-ik_e d} - r_{oe} e^{ik_e d}) \sin(\phi)}, t_{oe} = \frac{2k_o}{k_o + k_e}.$$
(18)

Substituting (18) into equation (10) one finds the profile of the resonant eigenmode within the ADL

$$E_x = \frac{A}{n_e} \sin(k_e z) \cos(\phi) - \frac{A}{n_e \zeta} \sin(k_o z) \sin(\phi),$$

$$E_y = \frac{A}{n_e} \sin(k_e z) \sin(\phi) + \frac{A}{n_e \zeta} \sin(k_o z) \cos(\phi).$$
(19)

The amplitude A has to be defined from a proper normalization condition. We mention that in limiting case $\phi \rightarrow 0$ the $\zeta \rightarrow \infty$ and fields $E_x = (A/n_e) \sin(k_e z)$, and $E_y = 0$ coincide with exact solution for BIC (8), (21) from our previous work³⁵. The obtained eigenfield are plotted in Fig. (1) (a). One can see that though the y-component is localized due to the band gap, the x-component grows with the distance from the ADL as it is typical for resonant eigenstates⁴.

3.4 Perturbative solution

Equations (16, 17) are generally not solvable analytically. There is, however, a single tractable perturbative solution in the case of quarter-wave optical thicknesses of the layers

$$k_o(\Lambda - d) = k_e d = \frac{k_o \lambda_{PBG}}{4} = \frac{\pi \omega}{2\omega_{PBG}},$$
(20)

where ω_{PBG} is the center frequency of photonic band gap, and λ_{PBG} is the corresponding wavelength. In our previous work³⁵ we found an exact solution for $\phi = 0$. Here by applying a Taylor expansion of equations (16, 17) in powers of the tilt angle ϕ we found approximate solutions for both resonant eigenfrequency and resonant eigenmode. By writing the resonant eigenfrequency as

$$\omega_r = \tilde{\omega} - i\gamma,$$
(21)

where both $\tilde{\omega}$ and γ are real and positive, and substituting into equations (16, 17) one finds

$$\tilde{\omega} = \omega_{PBG} + \frac{\omega_{PBG}}{\pi} q(1-q) \sin(\pi q) \cdot \phi^2 + \mathcal{O}(\phi^4)$$

$$\gamma = \frac{2\omega_{PBG}}{\pi} q(1-q) \cos^2(\pi q/2) \cdot \phi^2 + \mathcal{O}(\phi^4).$$
(22)

where $q = n_o/n_e$. Notice that the imaginary part of ω vanishes if $\phi = 0$. Thus, the system supports an antisymmetric BIC with the frequency $\omega_{BIC} = \omega_{PBG}$. That BIC was first reported in our previous work³⁵. We address the reader to the above reference for detailed analysis of the BIC and the plots visualizing its eigenfields. For the further convenience we also introduce the resonant vacuum wave number as

$$k_r = (\omega_r - i\gamma)/c = k_{BIC} [1 + \alpha \cdot \phi^2 + \mathcal{O}(\phi^4)],$$
(23)

where the complex valued α is implicitly defined by equation (22) and $k_{BIC} = \omega_{BIC}/c$. Finally, expanding (19) into the Taylor series in ϕ we find the following expression for the resonant eigenmode profile within the ADL

$$\mathbf{E}_r(z) = \frac{A}{n_e} \left\{ \begin{array}{l} \sin\left(\frac{\pi z}{2d}\right) + \mathcal{O}(\phi^2) \\ \left[\sin\left(\frac{\pi z}{2d}\right) + ie^{\frac{i\pi q}{2}} \sin\left(\frac{\pi qz}{2d}\right) \right] \cdot \phi + \mathcal{O}(\phi^3) \end{array} \right\}.$$
(24)

Notice that \mathbf{E}_r can be handled as 2×1 vector since $E_z = 0$.

3.5 Normalization condition

There are several equivalent formulations of the FV normalization condition^{30,36,38}. Here we follow³⁶, writing down the FV normalization condition through analytic continuation $\mathbf{E}(z, k)$ of the resonant eigenmode $\mathbf{E}_r(z)$ around the point $k = k_r$.

$$\int_{-d}^d \mathbf{E}_r \cdot \hat{\mathbf{e}} \mathbf{E}_r dz - \lim_{k \rightarrow k_r} \left\{ \frac{2[\mathbf{E}_r(d) \cdot \partial_z \mathbf{E}(d, k) - \mathbf{E}(d, k) \cdot \partial_z \mathbf{E}_r(d)]}{k_r^2 - k^2} \right\} = 1. \quad (25)$$

At the first glance the "flux" term in equation (25) differs from that in³⁶ by the factor of 2; this is because the "flux" term is doubled to account for both interfaces $z = \pm d$. For the resonant eigenmode $\mathbf{E}_r(z)$ found in the previous subsection the amplitude A corresponding equation (25) can be found analytically with the use of equation (24). This would, however, result in a very complicated expression. Fortunately, we shall see later on that in our case we do not need the general expression for A in the second order perturbative solution consistent with equation (22). By a close examination of equation (24) one can see that the Taylor expansion of A can only contain even powers of ϕ . Thus, for the further convenience we can write

$$A = \frac{1}{\sqrt{F + B \cdot \phi^2}} \quad (26)$$

assuming that F and B are such that the normalization condition (25) is satisfied up to $\mathcal{O}(\phi^4)$.

4 Scattering problem

Let us assume that a monochromatic y-wave is injected into the system through the left PhC arm. The scattering problem can now be solved through the following decomposition of the electric field within the ADL

$$\mathbf{E} = \mathbf{E}_{dir} + \mathbf{E}_{res}, \quad (27)$$

where the direct contribution is simply the electric field of the incident wave

$$\mathbf{E}_{dir} = \sqrt{I_0} e^{ik_0 z} \{0, 1\}^\dagger \quad (28)$$

with intensity I_0 , while \mathbf{E}_{res} can be viewed as the contribution due to the resonant pathway via excitation of the resonant eigenmode \mathbf{E}_r . Substituting Eq. (27) into Eq. (1) one obtains the inhomogeneous equation

$$\partial_z^2 \mathbf{E}_{res} + k_0^2 \hat{\mathbf{e}} \mathbf{E}_{res} = \mathbf{J} \quad (29)$$

with

$$\mathbf{J} = -\partial_z^2 \mathbf{E}_{dir} - k_0^2 \hat{\mathbf{e}} \mathbf{E}_{dir}. \quad (30)$$

Equation (29) can be solved with the use of Green's function

$$\mathbf{E}_{res}(z) = \int_{-d}^d \hat{\mathbf{G}}(z, z') \mathbf{J}(z') dz' \quad (31)$$

that is defined as the solution of Maxwell's equations with a delta source

$$\partial_z^2 \hat{\mathbf{G}}(z, z') + k_0^2 \hat{\mathbf{e}} \hat{\mathbf{G}}(z, z') = \delta(z - z') \hat{\mathbb{1}}_2, \quad (32)$$

where $\hat{\mathbb{1}}_2$ is the 2×2 identity matrix. According to³⁶ Green's function can be expanded into the orthonormal resonant eigenmodes as

$$\hat{\mathbf{G}}(z, z') = \sum_n \frac{\mathbf{E}_n(z) \otimes \mathbf{E}_n(z')}{2k_0(k_0 - k_n)}. \quad (33)$$

Of course we do not know the full spectrum k_n , since equations (16, 17) are not solved analytically. We, however, assume that the contribution of all eigenfields except \mathbf{E}_{res} is accumulated in the direct field. Thus, in the spectral vicinity of the quasi-BIC we apply the *resonant approximation* taking into account only the eigenmode associated with the BIC

$$\hat{\mathbf{G}}_{res}(z, z') = \frac{\mathbf{E}_r(z) \otimes \mathbf{E}_r(z')}{2k_0(k_0 - k_r)}. \quad (34)$$

The resonant field can now be calculated from equation (31) with the resonant Green's function equation (34) once the FV normalization condition (26) is applied to the quasi-BIC eigenmode. The analytic expression for the resonant field reads

$$\mathbf{E}_{res}(z) = \frac{1}{k_0(k_0 - k_r)(F + B \cdot \phi^2)\epsilon_e} \left[\frac{ik_0\sqrt{I_0}k_0^2(\epsilon_e - \epsilon_o)\cos(k_0d)}{k_o^2 - \pi^2/4d^2} \cdot \phi + \mathcal{O}(\phi^3) \right] \left\{ \begin{array}{l} \sin\left(\frac{\pi z}{2d}\right) \\ \left[\sin\left(\frac{\pi z}{2d}\right) + ie^{\frac{i\pi q}{2}} \sin\left(\frac{\pi qz}{2d}\right) \right] \cdot \phi \end{array} \right\}. \quad (35)$$

The above equation constitutes the perturbative solution of the scattering problem with the accuracy up to $\mathcal{O}(\phi^3)$. Notice

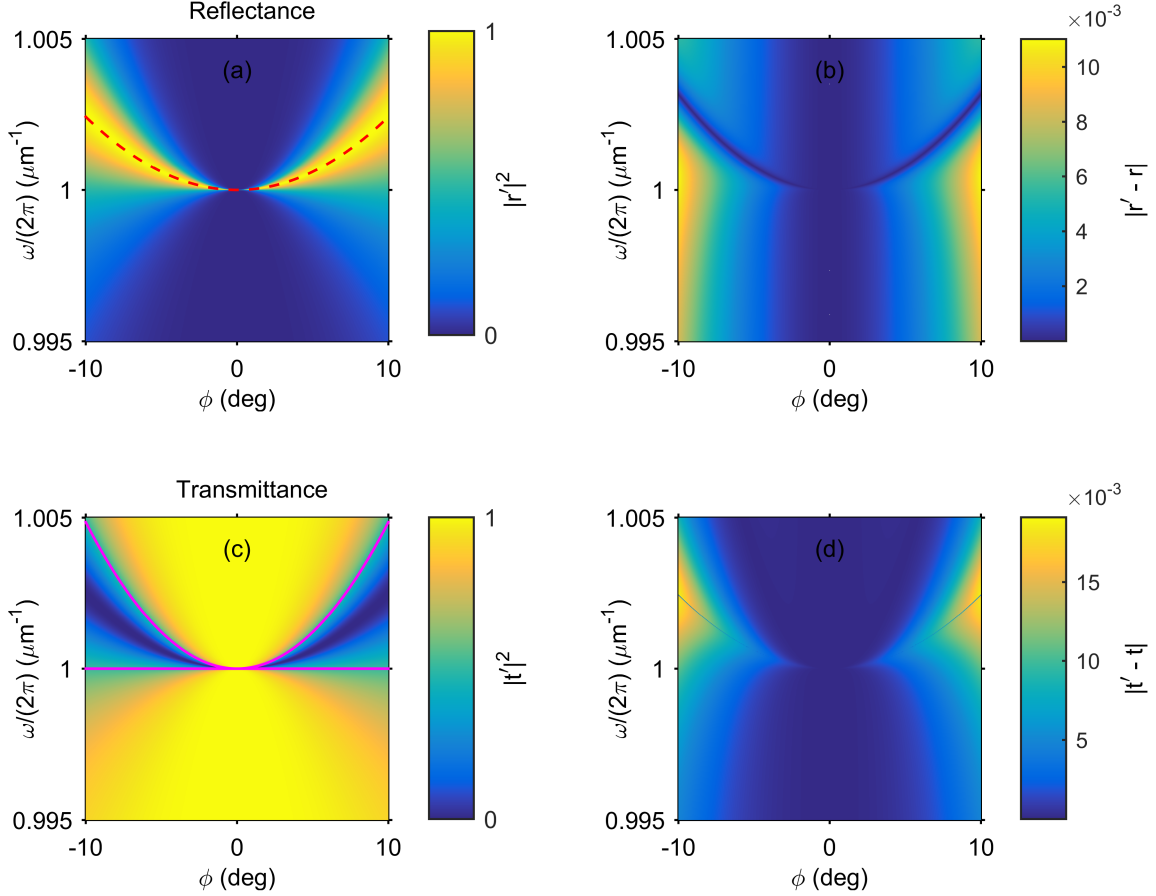


Figure 2. (a, c) The reflectance $|r'|^2$ (a) and transmittance $|t'|^2$ (c) spectra vs tilt angle ϕ of y-waves for PhC structure from Fig. 1(a) calculated with Berreman's method. The dashed red line shows the analytic resonant frequency $\omega_r/(2\pi)$ (22). The solid magenta lines show the analytic results for half-minima in transmittance $(\omega_r \pm \gamma)/(2\pi)$. (b, d) The difference between reflectance (b) and transmittance (d) spectra calculated with Berreman's method and analytically (38), (39). The parameters are the same as in Fig. 1.

that the terms dependant on B also vanish as $\mathcal{O}(\phi^3)$. Thus, in evaluating the FV normalization condition (25) we can restrict ourselves to $\phi = 0$ in which case the eigenmode is a BIC. Further on we safely set $B = 0$ in all calculations. The BIC is localized function decaying with $z \rightarrow \pm\infty$. Since the division into the scattering domain and the waveguides is arbitrary and the flux term is vanishing with $z \rightarrow \pm\infty$, one can rewrite the normalization condition for the BIC as follows

$$\int_{-\infty}^{\infty} \mathbf{E}_n \cdot \hat{\mathbf{e}} \mathbf{E}_n dz = 1. \quad (36)$$

We mention in passing that the equivalence between equations (25) and (36) can also be proven by subsequently applying the Newton-Leibniz axiom and Maxwell's equations (1) to the flux term in equation (25). The integral in equation (36) is nothing

but the energy stored in the eigenmode up to a constant prefactor. This integral for the system in Fig. 1(a) has been evaluated analytically in our previous work³⁵. As a result the normalization condition (36) yields

$$F = \frac{d}{1-q}. \quad (37)$$

Finally, the reflection and transmission coefficients can be found through the following equations, correspondingly

$$r = e^{-ik_0d} \mathbf{e}_y^\dagger \cdot \left[\mathbf{E}(-d) - \sqrt{I_0} e^{-ik_0d} \mathbf{e}_y \right], \quad (38)$$

and

$$t = e^{-ik_0d} \mathbf{e}_y^\dagger \cdot \mathbf{E}(d), \quad (39)$$

where $\mathbf{e}_y = \{0, 1\}^\dagger$ and \mathbf{E} is computed through equations (27, 28, 35). In Fig. 2 we compare the perturbative analytic solution against direct numerical simulations with the Berreman transfer-matrix method⁵⁴. One can see that deviation is no more than 2% even for relatively large angle $\phi = 10$ deg.

5 Conclusion

In this paper we considered light scattering by an anisotropic defect layer embedded into anisotropic photonic crystal in the spectral vicinity of an optical BIC. Using a resonant state expansion method we derived an analytic solution for reflection and transmission amplitudes. The analytic solution is constructed via a perturbative approach with the BIC as the zeroth order approximation. The solution is found to accurately describe the collapsing Fano feature in the spectral vicinity of the BIC. So far the theoretical attempts to describe the Fano feature induced by the BIC relied on phenomenological approaches such as the S -matrix approach⁴³, or the coupled mode theory⁴⁴. To the best of our knowledge this is the first full-wave analytic solution involving an optical BIC reported in the literature. We believe that the results presented offer a new angle onto the resonant state expansion method paving a way to analytic treatment of resonant scattering due to optical BICs. In particular we expect that the resonant approximation can be invoked to build a rigorous theory of nonlinear response⁵⁵. The BICs in photonic systems have already found important applications in enhanced optical absorption⁵⁶, surface enhanced Raman spectroscopy⁵⁷, lasing⁵⁸, and sensors⁵⁹. We speculate that analytic results are of importance for a further insight into localization of light as well as the concurrent phenomenon of collapsing Fano resonance.

References

1. Joannopoulos, J. D., Johnson, S. G., Winn, J. N. & Meade, R. D. *Photonic crystals: molding the flow of light* (Princeton university press, 2011).
2. Yang, Y. *et al.* Nonlinear fano-resonant dielectric metasurfaces. *Nano Lett.* **15**, 7388–7393, DOI: [10.1021/acs.nanolett.5b02802](https://doi.org/10.1021/acs.nanolett.5b02802) (2015).
3. Miroshnichenko, A. E., Flach, S. & Kivshar, Y. S. Fano resonances in nanoscale structures. *Rev. Mod. Phys.* **82**, 2257–2298, DOI: [10.1103/revmodphys.82.2257](https://doi.org/10.1103/revmodphys.82.2257) (2010).
4. Lalanne, P., Yan, W., Vynck, K., Sauvan, C. & Hugonin, J.-P. Light interaction with photonic and plasmonic resonances. *Laser & Photonics Rev.* **12**, 1700113, DOI: [10.1002/lpor.201700113](https://doi.org/10.1002/lpor.201700113) (2018).
5. Stratton, J. A. *Electromagnetic theory* (McGraw-Hill Book Company, Inc., 1941).
6. Haus, H. A. *Waves and Fields in Optoelectronics* (Prentice-Hall, Englewood Cliffs, NJ, 1984).
7. Fan, S., Suh, W. & Joannopoulos, J. D. Temporal coupled-mode theory for the Fano resonance in optical resonators. *J. Opt. Soc. Am. A* **20**, 569, DOI: [10.1364/josaa.20.000569](https://doi.org/10.1364/josaa.20.000569) (2003).
8. Suh, W., Wang, Z. & Fan, S. Temporal coupled-mode theory and the presence of non-orthogonal modes in lossless multimode cavities. *IEEE J. Quantum Electron.* **40**, 1511–1518, DOI: [10.1109/jqe.2004.834773](https://doi.org/10.1109/jqe.2004.834773) (2004).
9. Ruan, Z. & Fan, S. Temporal coupled-mode theory for fano resonance in light scattering by a single obstacle. *The J. Phys. Chem. C* **114**, 7324–7329, DOI: [10.1021/jp9089722](https://doi.org/10.1021/jp9089722) (2009).
10. Ruan, Z. & Fan, S. Temporal coupled-mode theory for light scattering by an arbitrarily shaped object supporting a single resonance. *Phys. Rev. A* **85**, 043828, DOI: [10.1103/physreva.85.043828](https://doi.org/10.1103/physreva.85.043828) (2012).

11. Rotter, I. A continuum shell model for the open quantum mechanical nuclear system. *Reports on Prog. Phys.* **54**, 635–682, DOI: [10.1088/0034-4885/54/4/003](https://doi.org/10.1088/0034-4885/54/4/003) (1991).
12. Dittes, F. The decay of quantum systems with a small number of open channels. *Phys. Reports* **339**, 215–316, DOI: [10.1016/s0370-1573\(00\)00065-x](https://doi.org/10.1016/s0370-1573(00)00065-x) (2000).
13. Ołowicz, J., Płoszajczak, M. & Rotter, I. Dynamics of quantum systems embedded in a continuum. *Phys. Reports* **374**, 271–383, DOI: [10.1016/s0370-1573\(02\)00366-6](https://doi.org/10.1016/s0370-1573(02)00366-6) (2003).
14. Chruściński, D. & Kossakowski, A. Feshbach projection formalism for open quantum systems. *Phys. Rev. Lett.* **111**, 050402, DOI: [10.1103/physrevlett.111.050402](https://doi.org/10.1103/physrevlett.111.050402) (2013).
15. Stöckmann, H.-J. *Quantum Chaos: An Introduction* (Cambridge University Press, Cambridge, U.K., 1999).
16. Pichugin, K., Schanz, H. & Šeba, P. Effective coupling for open billiards. *Phys. Rev. E* **64**, 056227, DOI: [10.1103/physreve.64.056227](https://doi.org/10.1103/physreve.64.056227) (2001).
17. Stöckmann, H.-J. *et al.* Effective hamiltonian for a microwave billiard with attached waveguide. *Phys. Rev. E* **65**, 066211, DOI: [10.1103/physreve.65.066211](https://doi.org/10.1103/physreve.65.066211) (2002).
18. Sadreev, A. F. & Rotter, I. S-matrix theory for transmission through billiards in tight-binding approach. *J. Phys. A: Math. Gen.* **36**, 11413–11433, DOI: [10.1088/0305-4470/36/45/005](https://doi.org/10.1088/0305-4470/36/45/005) (2003).
19. Savin, D., Sokolov, V. & Sommers, H.-J. Is the concept of the non-Hermitian effective hamiltonian relevant in the case of potential scattering? *Phys. Rev. E* **67**, 026215, DOI: [10.1103/physreve.67.026215](https://doi.org/10.1103/physreve.67.026215) (2003).
20. Maksimov, D. N., Sadreev, A. F., Lyapina, A. A. & Pilipchuk, A. S. Coupled mode theory for acoustic resonators. *Wave Motion* **56**, 52–66, DOI: [10.1016/j.wavemoti.2015.02.003](https://doi.org/10.1016/j.wavemoti.2015.02.003) (2015).
21. Racec, P. N., Racec, E. R. & Neidhardt, H. Evanescent channels and scattering in cylindrical nanowire heterostructures. *Phys. Rev. B* **79**, 155305, DOI: [10.1103/physrevb.79.155305](https://doi.org/10.1103/physrevb.79.155305) (2009).
22. Gongora, J. S. T., Favraud, G. & Fratallocchi, A. Fundamental and high-order anapoles in all-dielectric metamaterials via fano–feshbach modes competition. *Nanotechnology* **28**, 104001, DOI: [10.1088/1361-6528/aa593d](https://doi.org/10.1088/1361-6528/aa593d) (2017).
23. Lee, H. & Reichl, L. E. R-matrix theory with dirichlet boundary conditions for integrable electron waveguides. *J. Phys. A: Math. Theor.* **43**, 405303, DOI: [10.1088/1751-8113/43/40/405303](https://doi.org/10.1088/1751-8113/43/40/405303) (2010).
24. Schanz, H. Reaction matrix for dirichlet billiards with attached waveguides. *Phys. E: Low-dimensional Syst. Nanostructures* **18**, 429–435, DOI: [10.1016/s1386-9477\(03\)00147-4](https://doi.org/10.1016/s1386-9477(03)00147-4) (2003).
25. Berenger, J.-P. A perfectly matched layer for the absorption of electromagnetic waves. *J. Comput. Phys.* **114**, 185–200, DOI: [10.1006/jcph.1994.1159](https://doi.org/10.1006/jcph.1994.1159) (1994).
26. Chew, W. C. & Weedon, W. H. A 3D perfectly matched medium from modified Maxwell’s equations with stretched coordinates. *Microw. Opt. Technol. Lett.* **7**, 599–604, DOI: [10.1002/mop.4650071304](https://doi.org/10.1002/mop.4650071304) (1994).
27. Civitarese, O. & Gadella, M. Physical and mathematical aspects of gamow states. *Phys. Reports* **396**, 41–113, DOI: [10.1016/j.physrep.2004.03.001](https://doi.org/10.1016/j.physrep.2004.03.001) (2004).
28. More, R. M. Theory of decaying states. *Phys. Rev. A* **4**, 1782–1790, DOI: [10.1103/physreva.4.1782](https://doi.org/10.1103/physreva.4.1782) (1971).
29. Snyder, A. W. & Love, J. *Optical waveguide theory* (Springer Science & Business Media, 2012).
30. Muljarov, E. A., Langbein, W. & Zimmermann, R. Brillouin-Wigner perturbation theory in open electromagnetic systems. *EPL (Europhysics Lett.)* **92**, 50010, DOI: [10.1209/0295-5075/92/50010](https://doi.org/10.1209/0295-5075/92/50010) (2010).
31. Kristensen, P. T. & Hughes, S. Modes and mode volumes of leaky optical cavities and plasmonic nanoresonators. *ACS Photonics* **1**, 2–10, DOI: [10.1021/ph400114e](https://doi.org/10.1021/ph400114e) (2013).
32. Sauvan, C., Hugonin, J. P., Maksimov, I. S. & Lalanne, P. Theory of the spontaneous optical emission of nanosize photonic and plasmon resonators. *Phys. Rev. Lett.* **110**, DOI: [10.1103/physrevlett.110.237401](https://doi.org/10.1103/physrevlett.110.237401) (2013).
33. Hsu, C. W., Zhen, B., Stone, A. D., Joannopoulos, J. D. & Soljačić, M. Bound states in the continuum. *Nat. Rev. Mater.* **1**, 16048, DOI: [10.1038/natrevmats.2016.48](https://doi.org/10.1038/natrevmats.2016.48) (2016).
34. Koshelev, K., Favraud, G., Bogdanov, A., Kivshar, Y. & Fratallocchi, A. Nonradiating photonics with resonant dielectric nanostructures. *Nanophotonics* **8**, 725–745, DOI: [10.1515/nanoph-2019-0024](https://doi.org/10.1515/nanoph-2019-0024) (2019).
35. Timofeev, I. V., Maksimov, D. N. & Sadreev, A. F. Optical defect mode with tunable Q -factor in a one-dimensional anisotropic photonic crystal. *Phys. Rev. B* **97**, 024306, DOI: [10.1103/physrevb.97.024306](https://doi.org/10.1103/physrevb.97.024306) (2018).

36. Doost, M. B., Langbein, W. & Muljarov, E. A. Resonant state expansion applied to two-dimensional open optical systems. *Phys. Rev. A* **87**, 043827, DOI: [10.1103/physreva.87.043827](https://doi.org/10.1103/physreva.87.043827) (2013).
37. Doost, M. B., Langbein, W. & Muljarov, E. A. Resonant-state expansion applied to three-dimensional open optical systems. *Phys. Rev. A* **90**, 013834, DOI: [10.1103/physreva.90.013834](https://doi.org/10.1103/physreva.90.013834) (2014).
38. Muljarov, E. A. & Weiss, T. Resonant-state expansion for open optical systems: generalization to magnetic, chiral, and bi-anisotropic materials. *Opt. Lett.* **43**, 1978, DOI: [10.1364/ol.43.001978](https://doi.org/10.1364/ol.43.001978) (2018).
39. Tanimu, A. & Muljarov, E. A. Resonant-state expansion applied to one-dimensional quantum systems. *Phys. Rev. A* **98**, 022127, DOI: [10.1103/physreva.98.022127](https://doi.org/10.1103/physreva.98.022127) (2018).
40. Kim, C. S., Satanin, A. M., Joe, Y. S. & Cosby, R. M. Resonant tunneling in a quantum waveguide: Effect of a finite-size attractive impurity. *Phys. Rev. B* **60**, 10962 (1999).
41. Shipman, S. P. & Venakides, S. Resonant transmission near nonrobust periodic slab modes. *Phys. Rev. E* **71**, 026611 (2005).
42. Sadreev, A. F., Bulgakov, E. N. & Rotter, I. Bound states in the continuum in open quantum billiards with a variable shape. *Phys. Rev. B* **73**, 235342 (2006).
43. Blanchard, C., Hugonin, J.-P. & Sauvan, C. Fano resonances in photonic crystal slabs near optical bound states in the continuum. *Phys. Rev. B* **94**, 155303, DOI: [10.1103/physrevb.94.155303](https://doi.org/10.1103/physrevb.94.155303) (2016).
44. Bulgakov, E. N. & Maksimov, D. N. Optical response induced by bound states in the continuum in arrays of dielectric spheres. *J. Opt. Soc. Am. B* **35**, 2443, DOI: [10.1364/josab.35.002443](https://doi.org/10.1364/josab.35.002443) (2018).
45. Bogdanov, A. A. *et al.* Bound states in the continuum and fano resonances in the strong mode coupling regime. *Adv. Photonics* **1**, 1, DOI: [10.1117/1.ap.1.1.016001](https://doi.org/10.1117/1.ap.1.1.016001) (2019).
46. Foley, J. M., Young, S. M. & Phillips, J. D. Symmetry-protected mode coupling near normal incidence for narrow-band transmission filtering in a dielectric grating. *Phys. Rev. B* **89**, 165111, DOI: [10.1103/physrevb.89.165111](https://doi.org/10.1103/physrevb.89.165111) (2014).
47. Cui, X., Tian, H., Du, Y., Shi, G. & Zhou, Z. Normal incidence filters using symmetry-protected modes in dielectric subwavelength gratings. *Sci. Reports* **6**, 36066, DOI: [10.1038/srep36066](https://doi.org/10.1038/srep36066) (2016).
48. Doskolovich, L. L., Bezus, E. A. & Bykov, D. A. Integrated flat-top reflection filters operating near bound states in the continuum. *Photonics Res.* **7**, 1314, DOI: [10.1364/prj.7.001314](https://doi.org/10.1364/prj.7.001314) (2019).
49. Nguyen, T. G., Yego, K., Ren, G., Boes, A. & Mitchell, A. Microwave engineering filter synthesis technique for coupled ridge resonator filters. *Opt. Express* **27**, 34370, DOI: [10.1364/oe.27.034370](https://doi.org/10.1364/oe.27.034370) (2019).
50. Rytov, S. M. Electromagnetic properties of a finely stratified medium. *Sov. Phys. JETP* **2**, 466–475 (1956).
51. Yariv, A. & Yeh, P. *Optical waves in crystals*, vol. 5 (Wiley New York, 1984).
52. Shi, H. & Tsai, C.-h. Polariton modes in superlattice media. *Solid state communications* **52**, 953–954 (1984).
53. Camley, R. E. & Mills, D. L. Collective excitations of semi-infinite superlattice structures: Surface plasmons, bulk plasmons, and the electron-energy-loss spectrum. *Phys. Rev. B* **29**, 1695 (1984).
54. Berreman, D. W. Optics in stratified and anisotropic media: 4×4 -matrix formulation. *J. Opt. Soc. Am.* **62**, 502, DOI: [10.1364/josa.62.000502](https://doi.org/10.1364/josa.62.000502) (1972).
55. Bulgakov, E. N. & Maksimov, D. N. Nonlinear response from optical bound states in the continuum. *Sci. Reports* **9**, 7153, DOI: [10.1038/s41598-019-43672-y](https://doi.org/10.1038/s41598-019-43672-y) (2019).
56. Zhang, J. *et al.* Plasmonic focusing lens based on single-turn nano-pinholes array. *Opt. Express* **23**, 17883, DOI: [10.1364/oe.23.017883](https://doi.org/10.1364/oe.23.017883) (2015).
57. Romano, S. *et al.* Surface-enhanced raman and fluorescence spectroscopy with an all-dielectric metasurface. *The J. Phys. Chem. C* **122**, 19738–19745, DOI: [10.1021/acs.jpcc.8b03190](https://doi.org/10.1021/acs.jpcc.8b03190) (2018).
58. Kodigala, A. *et al.* Lasing action from photonic bound states in continuum. *Nature* **541**, 196–199, DOI: [10.1038/nature20799](https://doi.org/10.1038/nature20799) (2017).
59. Romano, S. *et al.* Label-free sensing of ultralow-weight molecules with all-dielectric metasurfaces supporting bound states in the continuum. *Photonics Res.* **6**, 726, DOI: [10.1364/prj.6.000726](https://doi.org/10.1364/prj.6.000726) (2018).

Acknowledgements

This work was supported by Russian Foundation for Basic Research project No. 19-52-52006. This project is also supported by the Higher Education Sprout Project of the National Chiao Tung University and Ministry of Education and the Ministry of Science and Technology (MOST No. 107-2221-E-009-046-MY3; No. 108-2923-E-009-003-MY3).

Author contributions statement

D.N.M. and T.I.V. conceived the idea presented. P.S.P. and D.N.M. have equally contributed to the analytic results. P.S.P. ran numerical simulations. D.N.M., P.S.P., K.P.C. and T.I.V. have equally contributed to writing the paper.

Additional information

Competing interests: The authors declare no competing interests.

Data availability: The data that support the findings of this study are available from the corresponding author, P.S.P., upon reasonable request.